https://doi.org/10.3311/PPee.14490

Periodica Polytechnica Electrical Engineering and Computer Science, 64(1), pp. 53–63, 2020

Robust Sliding Mode H∞ Controller of DFIG Based on Variable Speed Wind Energy Conversion System

Lakhdar Saihi[1,2*], Brahim Berbaoui[2], Hachemi Glaoui[1], Larbi Djilali[3], Slimani Abdeldjalil[2]

[1] Department of Electrical and Computer Engineering, University of Tahri Mohammed Bechar, P. O. B. 417, 08000 Bechar, Algeria
[2] Unité de Recherche en Energies Renouvelables en Milieu Saharien URERMS, Centre de Développement des Energies Renouvelables CDER, P. O. B. 478, 01000 Adrar, Alegria
[3] The Telecommunications, Signals and Systems Laboratory, University Amar Telidji, Route de Ghardaia, P. O. B. G37, 3000 Laghouat, Algeria
* Corresponding author, e-mail: saihi_lakhdar@urerms.dz

Received: 01 June 2019, Accepted: 11 September 2019, Published online: 24 October 2019

Abstract

In this study, a Sliding Mode (SM) methodology combined with a robust H∞ control scheme (SM-H∞) was proposed to control the stator active and reactive power generated by the Doubly Fed Induction Generator (DFIG). The purpose of the proposed controller is to improve the DFIG stator active and reactive power tracking performances by reducing chattering phenomena under variable wind speed, which provides major drawbacks of conventional SM controllers. The H∞ technique was used to define the SM attractive control part, which helps to reduce chattering phenomena and improves robustness in the presence of parameter variations and wind speed changing. The DFIG stator was directly connected to the grid and, its rotor was linked to the grid through a back-to-back converter. The proposed approach was tested using Matlab/Simulink and a comparison with the conventional SM and the SM fuzzy logic controllers was carried out. The results of simulation illustrated an effectiveness of the proposed SM-H∞ controller even in the presence of the DFIG parameter variations and speed changing compared with the other techniques.

Keywords

Doubly Fed Induction Generator (DFIG), H∞ control, Sliding Mode control, Wind Turbine

1 Introduction

The use of electric power generation as a renewable energy resources is becoming one of the ideal solutions used to resolve energy crises, environment pollution, and global warming [1]. Among different types of renewable energy resources, wind energy is one of the most used methods for power generation due to its economic benefits, and usefulness for power systems in diverse areas [2]. Recently, wind power generations have more attention for both industrial and academic researchers for improving performances of Wind Energy Conversion Systems (WECS) [3].

Doubly Fed Induction Generators (DFIGs) are widely used for variable speed wind system due to its benefits, such as the reduction of power converter size, possibility of stator active and reactive power control independently, and decoupling between mechanical speed and grid frequency [4]. The most known electric configuration for the DFIG based Wind Turbine (WT) is when the DFIG stator is linked directly to the grid, its rotor is connected to the grid via back-to-back power converter [5]; this configuration ensures the energy generation at nominal grid voltage and frequency values independently of mechanical speed changes [6].

In the context of DFIG control, various control techniques have been developed for Variable Speed Wind Turbine (VSWT) based on DFIG. The most popular one was named decoupled Proportional-Integral (PI) controller [7], where the Field Oriented Control (FOC) combined with the PI controller was used to regulate the stator active and reactive power [4, 8]. However, this controller is not robust and highly depends on the DFIG parameters, which affects electrical power generation quality [9].

In the last years, Sliding Mode (SM) control has been extensively tested due to its implementation simplicity and robustness respecting of some classes of system uncertainties and external disturbances, which can affect the trajectories tracking of the controlled systems [10, 11]. Different studies have been published for the DFIG control scheme

Cite this article as: Saihi, L., Berbaoui, B., Glaoui, H., Djilali, L., Abdeldjalil, S. "Robust Sliding Mode H∞ Controller of DFIG Based on Variable Speed Wind Energy Conversion System", Periodica Polytechnica Electrical Engineering and Computer Science, 64(1), pp. 53–63, 2020. https://doi.org/10.3311/PPee.14490

using the SM control. In [12], a conventional SM control was used to regulate the DFIG stator active and reactive power, where the proposed controller was compared with the PI-FOC and the Reference Signal Tracking (RST) controllers, the SM controller in this work shows a high performances compared with the PI and the RST controllers, but it does not treat the SM chattering problem caused by attractive control part [13, 14], these chattering phenomena my leads to an instability of system [15].

Furthermore, previous studies were carried out to improve the SM technique drawbacks and reduce chattering phenomena effects, the development of robust controller is very important. The fuzzy logic control is one of the important branches of artificial intelligence strategies that is able to reproduce human reasoning and occupies a large place in modern research fields [16]. This technique becomes very dominant in several industrial fields. The integration neuro-fuzzy is also an interesting and present a strong solution to ensure optimal regulation that meets the requirements of the user even in a difficult and variable environment [16, 17].

Melin and Castillo in [18] have proposed to hybrid neuro with fuzzy logic for controlling the battery charging process. For the combination of SM, author in [19] and in [20] proposed a SM controller combined with fuzzy logic technique, which was applied to control the variable speed WECS based on a DFIG; this study leads to reduce the SM chattering phenomena; however, the obtain results mentioned that a significant ripples are still observed on the controlled dynamics. In another study in [11], where a SM fuzzy logic controller was used to control the stator powers generated by a DFIG; the simulation results mentioned that the response time is significantly reduced compared with the convectional controllers with limitation of disturbances effects. However, chattering is still observed on the stator active and reactive power dynamics. In [21], an H∞ controller is proposed to control the DFIG active and reactive power, the obtained results illustrated that the proposed H∞ controller improves tracking performances compared with the decoupled PI controller. Previous research has established that the role of the robust H∞ controller designed for the DFIG to improve quality of generated power by reducing the stator currents harmonics [22].

This study proposed the SM-H∞ controller for the DFIG stator active and reactive power. The proposed controller leads to reduce chattering phenomena presented in conventional SM controllers caused by attractive control part. To reach this objective, the H∞ was used to define the attractive control part of the SM control methodology. This modified SM control algorithm (SM-H∞) was considered as the main contribution of this research. The simulation results illustrated the effectiveness of the proposed controller for chattering reduction in comparisons with the conventional SM and the SM fuzzy logic controllers. In addition, the proposed control algorithm reached an adequate tracking performances in presence of parameter variations and wind speed changes.

2 Wind power system model

The selected wind power system is based on a DFIG. As known, the wind system is composed of two parts: mechanical and electrical. The mechanical part is the aero-generator used to extract power from wind. Moreover, the electrical part is composed of DC-link and DFIG then used to converter the generated mechanical power to electrical energy. Fig. 1 displays the WT system based on DFIG. The DFIG

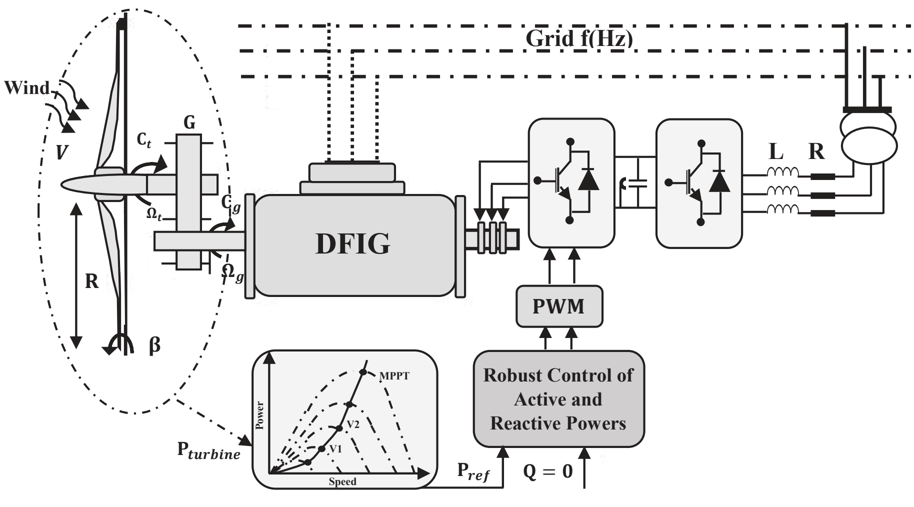

Fig. 1 DFIG based Wind Turbine system.

stator is directly linked to grid, whereas the rotor is connected to grid through a back-to-back converter controlled by Pulse Width Modulation (PWM) [6]. This back-to-back converter is composed of two voltage sources converters which are: the Rotor Side Converter (RSC) and the Grid Side Converter (GSC) [23, 11].

In this study, the DFIG active and reactive power are controlled via the RSC controller, while the GSC controller was not included and the DC voltage at the output of the DC link was considered as a constant. In order to establish the RSC controller, the SM-H∞ controller was suggested as a controller to improve the DFIG control performances and reduce chattering phenomena presented in the conventional SM controllers [11].

2.1 DFIG modelling

The DFIG model in $d-q$ reference frame was given by Eq. (1) [24, 25]:

$$\begin{cases} v_{ds} = R_s i_{ds} + \dfrac{d\varphi_{ds}}{dt} - \omega_s \varphi_{qs} \\ v_{qs} = R_s i_{qs} + \dfrac{d\varphi_{qs}}{dt} + \omega_s \varphi_{ds} \\ v_{dr} = R_r i_{dr} + \dfrac{d\varphi_{dr}}{dt} - (\omega_s - \omega_r)\varphi_{qr} \\ v_{qr} = R_r i_{qr} + \dfrac{d\varphi_{qr}}{dt} - (\omega_s - \omega_r)\varphi_{dr} \end{cases} . \tag{1}$$

The flux linkage equation is:

$$\begin{cases} \varphi_{ds} = l_s i_{ds} + l_m i_{dr} \\ \varphi_{qs} = l_s i_{qs} + l_m i_{qr} \\ \varphi_{dr} = l_r i_{dr} + l_m i_{ds} \\ \varphi_{qr} = l_r i_{qr} + l_m i_{qs} \end{cases} . \tag{2}$$

Where l_s and l_r are the stator and the rotor inductances (H) respectively, l_m is the mutual inductance (H), i_{ds}, i_{qs}, i_{dr} and i_{qr} are the $d-q$ stator and rotor currents (A), R_s, R_r are the stator and the rotor resistances (Ω) respectively, p is the number of pole pairs; φ_{ds}, φ_{qs}, φ_{dr} and φ_{qr} are the $d-q$ stator and rotor flux (Web) respectively. The v_{ds}, v_{qs}, v_{dr} and v_{qr} are the $d-q$ stator and the rotor voltages (V) respectively.

The expression of the electromagnetic torque is [13, 19]:

$$T_{em} = p \frac{l_m}{l_s} \left(\varphi_{qs} i_{dr} - \varphi_{ds} i_{qs} \right). \tag{3}$$

The active (P_s) and reactive (Q_s) stator power are [24, 25]:

$$\begin{cases} P_s = v_{ds} i_{ds} + v_{qs} i_{qs} \\ Q_s = v_{qs} i_{ds} - v_{ds} i_{qs} \end{cases} . \tag{4}$$

2.2 DFIG Field Oriented Control

From Eq. (3) and Eq. (4), a high coupling between the stator and the rotor components was presented, which influenced the role of DFIG control to be particularly difficult. In order to ensure the decoupling between control axes, a Field Oriented Control (FOC) technique was applied [23, 24] by aligning the stator flux φ_s with the direct axis $-d-$, as shown in Fig. 2, then [26, 27]:

$$\begin{cases} \varphi_{ds} = \varphi_s \\ \varphi_{qs} = \dfrac{d\varphi_{qs}}{dt} = 0 \end{cases} \Rightarrow \begin{cases} v_{ds} = 0 \\ v_{qs} = v_s = \omega_s \varphi_s \end{cases}$$

and

$$\begin{cases} \varphi_s = l_s i_{ds} + l_m i_{dr} \\ 0 = l_s i_{qs} + l_m i_{qr} \end{cases} . \tag{5}$$

Thus, the electromagnetic torque becomes [11, 19]:

$$T_{em} = -p \left(\varphi_s \frac{l_m}{l_s} i_{qr} \right), \tag{6}$$

and the stator active and reactive power were expressed by Eq. (7) [11, 19]:

$$\begin{cases} P_s = -v_s \dfrac{l_m}{l_s} i_{qr} \\ Q_s = -v_s \dfrac{l_m}{l_s} i_{dr} + \dfrac{v_s^2}{l_s \omega_s} \end{cases} . \tag{7}$$

The DFIG control stator powers is achieved through the control of the DFIG rotor currents. For that, a relationship between the rotor currents and the rotor voltages was established by Eq. (8) [13, 14]:

$$\begin{cases} v_{dr} = R_r i_{dr} + l_r \sigma \dfrac{di_{dr}}{dt} - (g\omega_s l_r \sigma i_{qr}) \\ v_{qr} = R_r i_{qr} + l_r \sigma \dfrac{di_{qr}}{dt} + (g\omega_s l_r \sigma i_{dr}) + g \dfrac{l_m v_s}{l_s} \end{cases} . \tag{8}$$

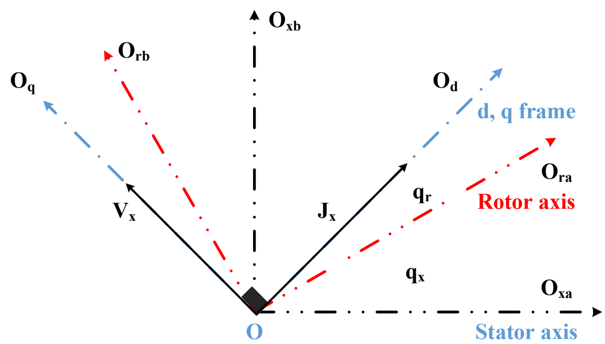

Fig. 2 Orientation $d-q$ reference frame [11].

Where $\sigma = \left(1 - \frac{l_m^2}{l_s l_r}\right)$ represents the dispersion coefficient. The Fig. 3 depicted the DFIG active and reactive power control scheme based on Sliding Mode Field Oriented Control (SM-FOC), where two independent controllers are used for each control axis. This method focused on compensating the linking terms between the $d-q$ axes $(g\omega_s l_r \sigma i_{qr})$, $(g\omega_s l_r \sigma i_{dr})$ and the disturbance term $\left(g\frac{l_m v_s}{l_s}\right)$ on the $-q-$ axis in Eq. (8) to ensure an independent control for the stator active and reactive powers.

3 DFIG proposed control strategy

Recently, there has been an increasing interest in the use of DFIG Sliding Mode control due to its robustness to the parameter of variations and disturbances under matching condition [28, 29].

The SM controller was designed to force the controlled dynamics towards sliding surface and keeps it there [30]. In order to force the DFIG stator active and reactive power to track their corresponding references, the sliding surfaces are selected to equal the error between the desired dynamics and real ones by Eq. (9) [31]:

$$\begin{cases} S(P) = \left(P_s^{ref} - P_s\right) \\ S(Q) = \left(Q_s^{ref} - Q_s\right) \end{cases}. \tag{9}$$

The sliding surface derivative was calculated by substituting the active and reactive power expressions of Eq. (7) in Eq. (9) by Eq. (10) [11, 19]:

$$\begin{cases} \dot{S}(P) = \left(\dot{P}_s^{ref} + v_s \frac{l_m}{l_s} \dot{i}_{qr}\right) \\ \dot{S}(P) = \left(\dot{Q}_s^{ref} + v_s \frac{l_m}{l_s} \dot{i}_{dr}\right) \end{cases}. \tag{10}$$

Using the current expressions i_{qr} and i_{dr} obtained from the voltage v_{qr} and v_{dr} of Eq. (8) in Eq. (10) we obtain [11]:

$$\begin{cases} \dot{S}(P) = \dot{P}_s^{ref} + v_s \frac{l_m}{l_s l_r \sigma}\left(v_{qr} - R_r i_{qr}\right) \\ \dot{S}(Q) = \dot{Q}_s^{ref} + v_s \frac{l_m}{l_s l_r \sigma}\left(v_{dr} - R_r i_{dr}\right) \end{cases}. \tag{11}$$

Replacing v_{qr} by $v_{qr}^{eq} + v_{qr}^{n}$ and v_{dr} by $v_{dr}^{eq} + v_{dr}^{n}$ in Eq. (11), the sliding surface derivatives can be rewritten by Eq. (12):

$$\begin{cases} \dot{S}(P) = \dot{P}_s^{ref} + v_s \frac{l_m}{l_s l_r \sigma}\left(\left(v_{qr}^{eq} + v_{qr}^{n}\right) - R_r i_{qr}\right) \\ \dot{S}(Q) = \dot{Q}_s^{ref} + v_s \frac{l_m}{l_s l_r \sigma}\left(\left(v_{dr}^{eq} + v_{dr}^{n}\right) - R_r i_{dr}\right) \end{cases}. \tag{12}$$

The equivalent control is obtained by using the following condition [31]:

$$\begin{cases} S(P) = 0 \rightarrow \dot{S}(P) = 0,\ v_{qr}^{n} = 0 \\ S(Q) = 0 \rightarrow \dot{S}(Q) = 0,\ v_{dr}^{n} = 0 \end{cases}. \tag{13}$$

Then, the expression of the equivalent control is calculated as:

$$\begin{cases} v_{qr}^{eq} = -\dot{P}_s^{ref} \frac{l_s l_r \sigma}{v_s l_m} + R_r i_{qr} \\ v_{dr}^{eq} = -\dot{Q}_s^{ref} \frac{l_s l_r \sigma}{v_s l_m} + R_r i_{dr} \end{cases}. \tag{14}$$

During the convergence mode, the condition $S(P)\dot{S}(P) \le 0$ and $S(Q)\dot{S}(Q) \le 0$ are verified and the equivalent control was applied. Substituting Eq. (14) in Eq. (12), the sliding surfaces derivatives are obtained as [30, 31]:

$$\begin{cases} \dot{S}(P) = -v_s \frac{l_m}{l_s l_r \sigma} v_{qr}^{n} \\ \dot{S}(Q) = -v_s \frac{l_m}{l_s l_r \sigma} v_{dr}^{n} \end{cases}. \tag{15}$$

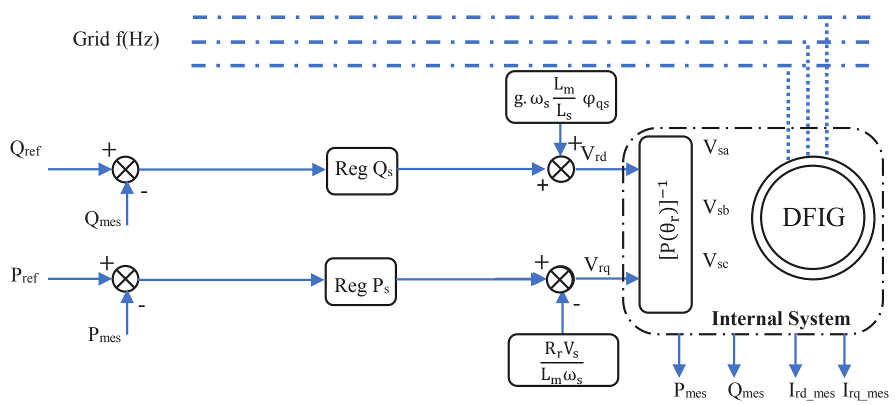

Fig. 3 Global control structure of the wind generator with DFIG.

To define v_{qr}^n and v_{dr}^n controls which are considered as an attractive control part of the SM controller, it is often selected as a relay shape defined as [14, 19]:

$$\begin{cases} v_{qr}^n = -K_P \dfrac{V_s l_m}{l_s l_r} \sigma sign(S(P)) \\ v_{dr}^n = -K_Q \dfrac{V_s l_m}{l_s l_r} \sigma sign(S(Q)) \end{cases}. \quad (16)$$

The K_P and K_Q should be positive gains [29, 31]. Considering the nature of attractive control part, chattering phenomena was produced and can destabilize the plant.

3.1 Sliding Mode H∞ controller

The attractive control part of the SM algorithm causes chattering phenomena. In order to avoid this drawback, H∞ was proposed to design an attractive control part. For that, the SM control law was defined by including H∞ technique by Eq. (17):

$$v = v_{eq} + v_{H\infty} \Rightarrow \begin{cases} v_{qr} = v_{qr}^{eq} + v_{qr}^{H\infty} \\ v_{dr} = v_{dr}^{eq} + v_{dr}^{H\infty} \end{cases}. \quad (17)$$

The suggested control scheme is a hybrid control including the SM control and robust H∞ control, where the switching controller term, $K_P sign(S(P))$ and $K_Q sign(S(Q))$ are defined by using the H∞ control technique. Fig. 4 explains the SM-H∞ control structure.

Robust H∞ control issue has been examined widely in recent years [32, 33]. It is an important solution for system disturbances and uncertainties [34].

The main problem of the H∞ control technique is to find the controller function $K(s)$, which internally stabilizing the controlled dynamics closed-loop, and minimizing the H∞ norm of the transfer function as depicted in Fig. 4, which express the relation between input and output [22, 35]:

$$\left\| \begin{matrix} W_1(s)S(s) & W_1(s)W_3(s)S(s)G(s) \\ W_2(s)K(s)S(s) & W_2(s)K(s)W_3(s)S(s)G(s) \end{matrix} \right\|_\infty < \gamma. \quad (18)$$

With γ is a positive constant value named optimization level. $S(s)$ is the sensitivity function calculated as $S(s) = \dfrac{1}{1+G(s)K(s)}$ [21, 22].

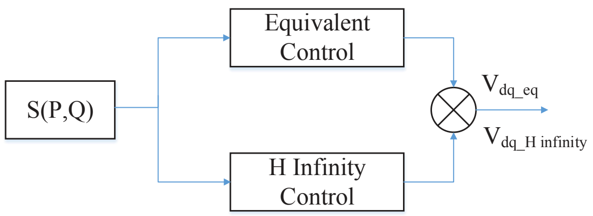

Fig. 4 Sliding mode H∞ controller.

The standard configuration of the H∞ controller $K(s)$ represented by a multi-variable model with two inputs and two outputs, the plant $G(s)$ and the uncertainties W_n is illustrated in Fig. 5 [36, 37].

Where $z(t)$ is the criterion H∞ input vector, $y(t)$ is the measured output vector, $u(t)$ is the control input vector, and $W_n(s)$ is the exogenous input vector [35].

Fig. 6 shows the whole control system based on SM-H∞ controller where the proposed control scheme was augmented by the weighting function [38, 39].

For the SM-H∞ controller, where H∞ technique is selected to compose an attractive control part, two feedback controls loops are designed; the first one is used to regulate the stator active power and the second one is utilized for adjusting the stator reactive power. The nominal system $G(s)$ is augmented with weighting transfer functions $W_1(s)$, $W_2(s)$ and $W_3(s)$ penalizing the error signals, the control signals, and output signals respectively.

The robustness improvement of the H∞ control is mainly based on the correct selection of the proper weighting functions as a poor selection weights definitely leads to inappropriate system performances.

3.2 Weighting functions selection

In order to define sensitivity the function $S(s)$ using weighting function $W_1(s)$, the following condition should be required:

$$\|W_1(s)S(s)\|_\infty \le \gamma. \quad (19)$$

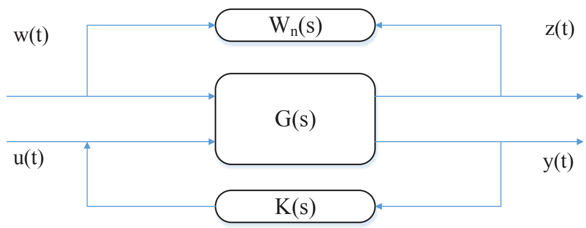

Fig. 5 General setup of the H∞ design problem.

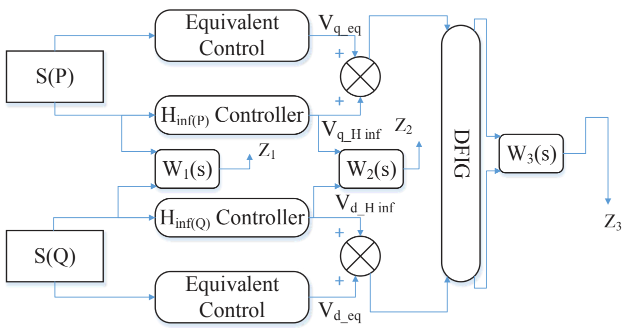

Fig. 6 Mixed sensitivity scheme for robust control design.

Where $W_1(s)$ is defined as $W_1(s)=\frac{s/M_s+\omega_b}{s+\omega_b\varepsilon}$ to ensure an adequate selection of weighting function $W_1(s)$.

The parameter ε is selected to be a low value at base frequencies and M_s is fixed at maximum limit value in high frequencies of the sensitivity function $S(s)$ of response frequency as illustrated in Fig. 7.

To determine the function $K(s)S(s)$, weighting function $W_2(s)$ is used and the following condition should be required [36, 38]:

$$\|W_2(s)K(s)S(s)\|_\infty \le \gamma. \quad (20)$$

Where $W_2(s)$ defined as $W_2(s)=\frac{s+\frac{\omega_{bc}}{M_s}}{s\varepsilon_1+\omega_{bc}}$. To assure an adequate selection of the weighting function $W_2(s)$, ε_1 and M_s are chosen with same manner as in $W_1(s)$ but the frequency response of the function $K(s)S(s)$ was considered, as depicted in Fig. 8.

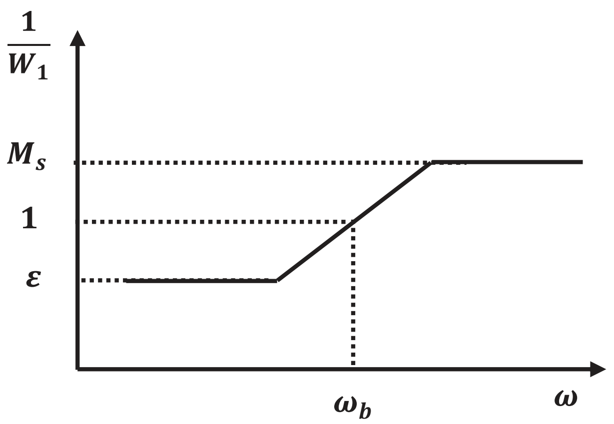

Fig. 7 Weighting function $1/W_1(s)$.

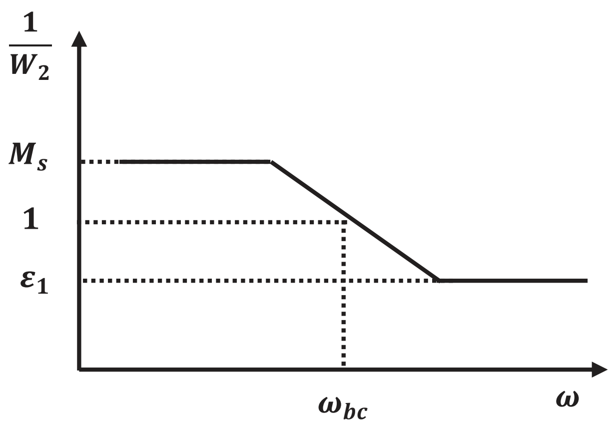

Fig. 8 Weighting function $1/W_2(s)$.

The function $S(s)G(s)$ depends on the two filters $W_1(s)$ and $W_3(s)$. To ensure the stability of the controlled system, the following condition was considered [21, 35]:

$$\|W_1(s)S(s)G(s)W_3(s)\|_\infty \le \gamma. \quad (21)$$

In general case, it is sufficient to fixed $W_3(s)$ as a constant, which permits to adjust the behavior of $S(s)G(s)$ in low and medium frequencies, and prove the correct behavior in presence of disturbances [36, 38].

Fig. 9 presents the sensitivity function $S(s)$, complementary sensitivity functions $T(s)=S(s)G(s)$ and $S(s)K(s)$. Those functions are given for system without uncertainties. For the system with uncertainties, functions are given by inverse of weighting function of $\frac{\gamma}{W_1(s)}$, $\frac{\gamma}{W_2(s)}$ and $\frac{\gamma}{W_1(s)W_3(s)}$. It is very clear to observe the infinity norm of the condition (Eq. (18)) which is lower than γ, the sensitivity and complementary sensitivity functions ensures an adequate attenuation of noise and disturbances rejection.

We therefore conclude that $\gamma_P=0.3271$ and $\gamma_Q=0.5482$. The Sliding Mode of attractive control part resulted from the H∞ technique is obtained by Eqs. (22), (23) for the active and reactive power respectively:

$$v_{qrn}=K_Q(s)=\frac{1.232\cdot10^6\ s^2+1.371\cdot10^{10}\ s+9.631\cdot10^{11}}{s^3+2.052\cdot10^{10}\ s^2+2.27\cdot10^{14}\ s+3.038\cdot10^{13}} \quad (22)$$

$$v_{drn}=K_P(s)=\frac{5.38\cdot10^6\ s^2+5.99\cdot10^{10}\ s+4.207\cdot10^{12}}{s^3+5.955\cdot10^7\ s^2+6.587\cdot10^{11}\ s+8.813\cdot10^{10}}. \quad (23)$$

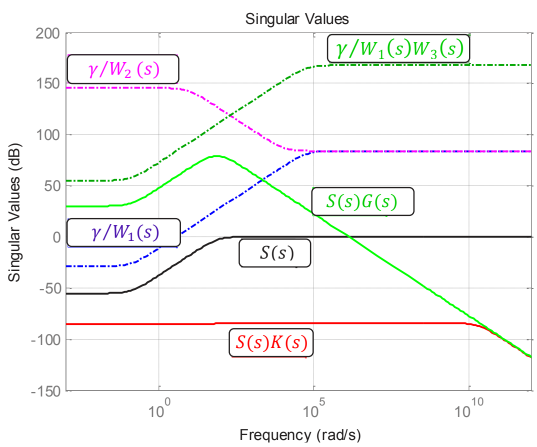

Fig. 9 Frequency response of sensitivities and weightings functions.

4 Simulation results

The proposed SM-H∞ controller as applied for the DFIG stator active and reactive power has been implemented using Matlab/Simulink[1]. In addition, a comparison study between the proposed controller with the SM conventional and the SM fuzzy logic controllers was carried out into account in terms of trajectory tracking (reactive and active power), chattering phenomena reduction, wind speed changing and robustness to DFIG parameter variations (parameters of Wind Turbine and DFIG are given in Table 1 and Table 2).

Fig. 10 presents the selected wind profile as applied to the Wind Turbine; the wind speed changes between 9.5 m/s and 11.5 m/s.

The DFIG rotor mechanical speed was displayed in Fig. 11 where a time-varying mechanical speed was applied to the DFIG, which improve the analyze of the impact of WT speed variations on the stator active and reactive power.

The generated active power measured by the DFIG stator and controlled by the proposed SM-H∞ (red) as well as the conventional SM (blue), and the SM fuzzy logic (green) controllers was depicted in Fig. 12. The active power desired by dynamics (black) was selected as a time-varying trajectory in order to examine the proposed controller performances in presence of reference variations.

Fig. 13 offers the behavior of the stator reactive power controlled by the proposed SM-H∞ (red), the conventional SM (blue), and the SM fuzzy logic (green) controllers where its desired value (black) was maintained null in order to obtain the stator power factor at unit value.

Fig. 14 (a) and (b) shows the DFIG electromagnetic torque behavior and stator current. Simulation results show the effectiveness of the proposed controller to track the time-varying active power for desired reference and maintain constant the stator reactive power. In addition, chattering phenomena is largely reduced by the proposed SM-H∞ compared with the other controller (convectional SM and SM fuzzy logic), which helps to avoid major drawbacks of the SM control algorithm. It's also ensure the stability of the controlled dynamics, and improve control scheme performances. Moreover, the proposed SM-H∞ ensures high decoupling between the control $d-q$ axes compared with the other controllers.

As a result, the proposed SM-H∞ controller illustrated an adequate tracking performances even in the presence of reference variations and speed changing. In addition, the response time was improved and chattering phenomena was largely reduced, which helps to improve the quality of the generated power.

Table 1 Parameters of wind turbine

Radius of wind turbine	35.25 m
Number of blades	3
Nominal rotational speed	10 m/s
Optimum power coefficient constant	8.1
Maximum *Cp*	0.42
Density of air	1.225 kg m^{-3}
Dry friction torque	953 N m
Total inertia of the mechanical	50 kg m^2

Table 2 Parameters of the DFIG

Rated generator power	1.5 MW
Rated voltage	698 V
Rated mechanical speed	12 m/s
Rated frequency	50 Hz
Pole pairs	2
PM flux	0.0024 Wb
Stator *D*-axis inductance	0.0136 H
Rotor *Q*-axis inductance	0.0137 H
Mutual inductance	0.0135 H
Stator resistance	0.012 Ω
Rotor resistance	0.021 Ω

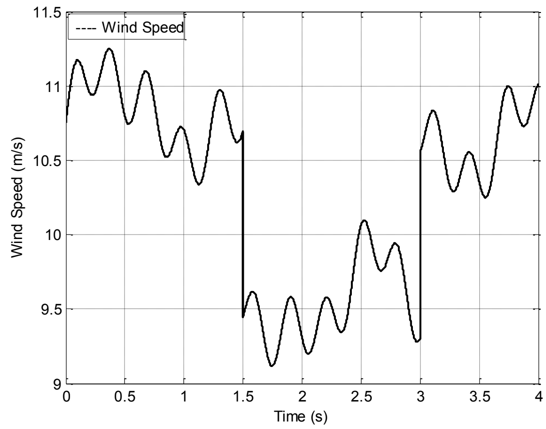

Fig. 10 Wind speed profile.

4.1 Robustness test

The purpose of this test is to examine the proposed controller performances and compare it with the conventional SM and SM fuzzy logic controllers. To reach this objective, the DFIG electric parameters were changed as follows.

Fig. 15 presented the DFIG stator active power with a change of the rotor resistance R_r by 200 % of its nominal value. The DFIG stator reactive behavior with an

1 Matlab, Simulink. de 1994-2019, © The Math Works, Inc.

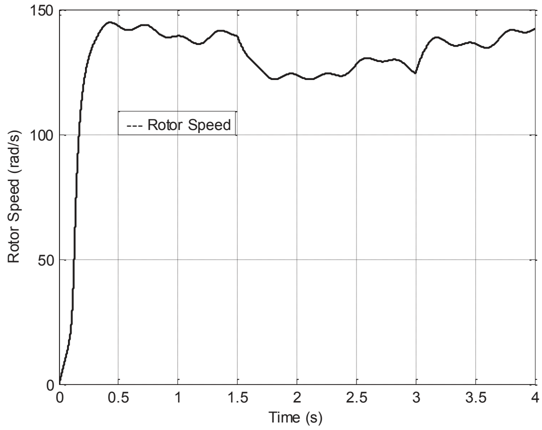

Fig. 11 DFIG rotor speed.

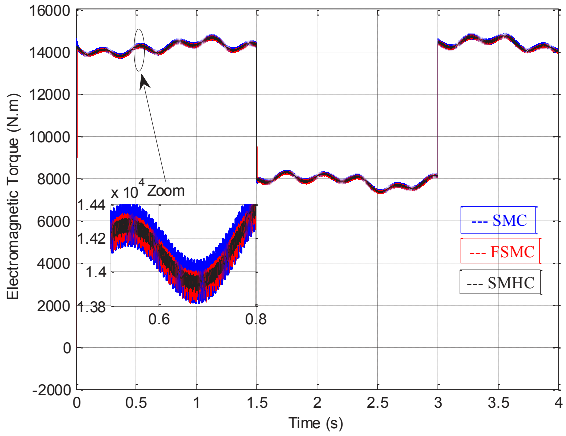

(a)

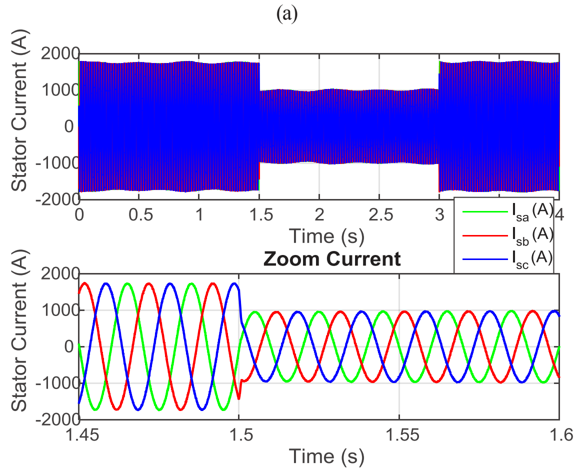

(b)

Fig. 14 (a) DFIG electromagnetic torque, with SMC and SM Fuzzy and SM-H∞ controllers. (b) DFIG stator current with SM-H∞ controller.

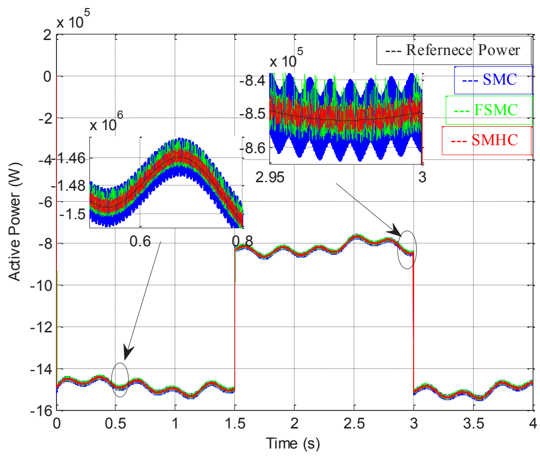

Fig. 12 DFIG active power with SMC, SM Fuzzy and SM-H∞ controllers.

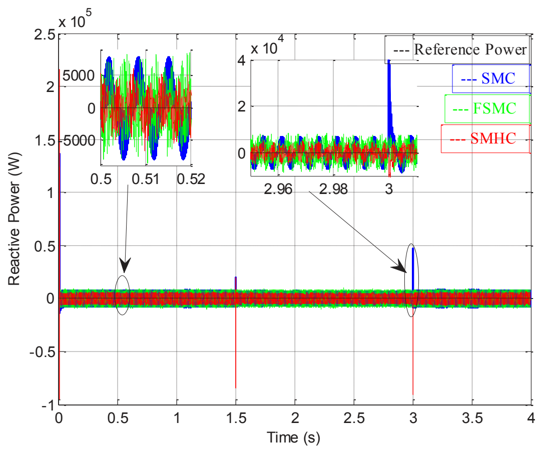

Fig. 13 DFIG reactive power with SMC, SM Fuzzy and SM-H∞ controllers.

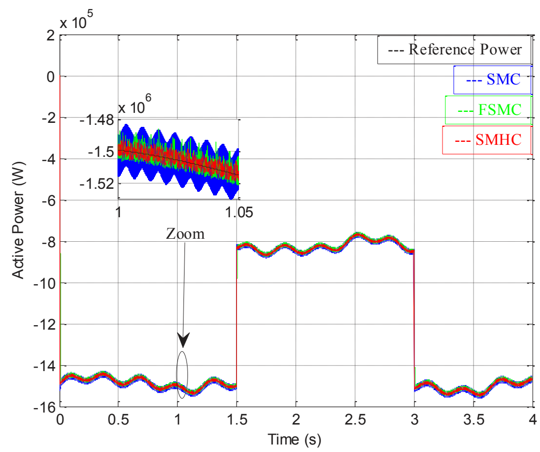

Fig. 15 The rotor resistance R_r variation effects on active power.

augmentation of the rotor resistance R_r by 200 % of its nominal value as illustrated in Fig. 16.

Fig. 17 shown the DFIG stator active and reactive power with a variation of the stator resistance R_r by 150 % of its nominal value.

Fig. 18 displayed the behavior of the DFIG stator active power with an increase of the rotor inductance l_r by 100 % of its nominal value. The DFIG stator reactive power dynamics with an enlargement of the rotor inductance l_r by 100 % of its nominal value shown in Fig. 19.

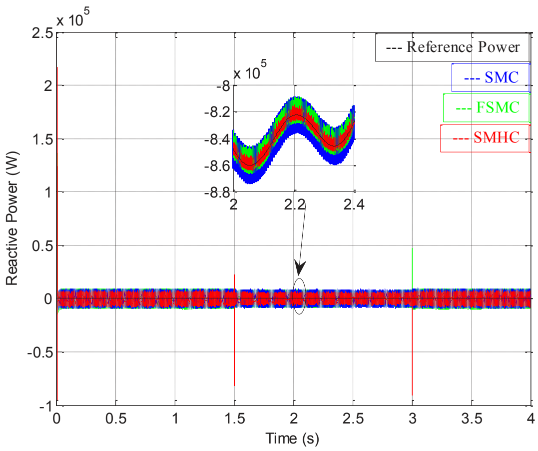

Fig. 16 The rotor resistance R_r variation effects on reactive power.

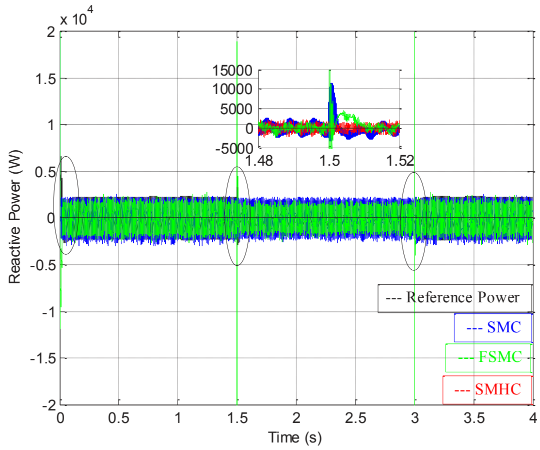

Fig. 19 The rotor inductance l_r variation effects on reactive power.

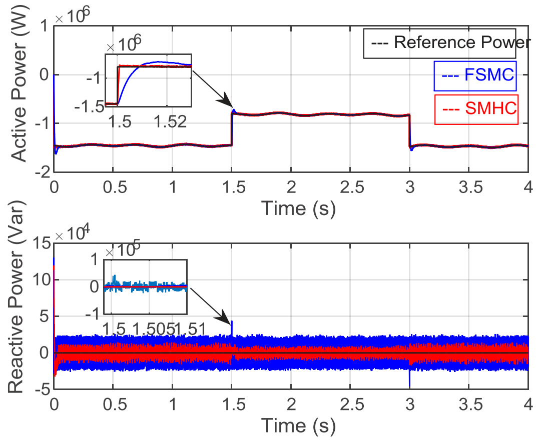

Fig. 17 Stator resistance R_r variation effects on active/reactive power.

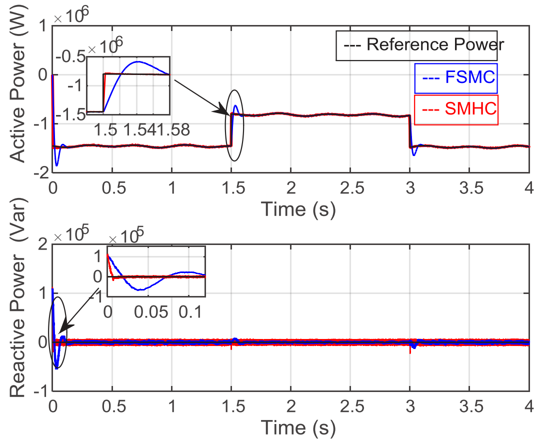

Fig. 20 Stator inductance l_s variation effects on active/reactive power.

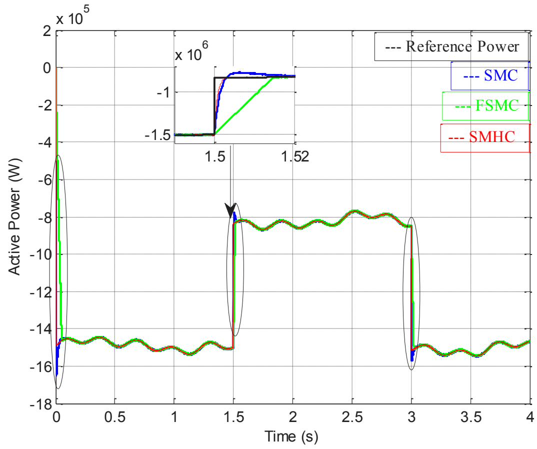

Fig. 18 The rotor inductance l_r variation effects on active power.

Fig. 20 presented the DFIG stator active and reactive power with an augmentation of the stator inductance L_s by 100 % of its nominal value.

Consequently, it can be seen that the DFIG rotor parameter variations has no effects on the stator active and reactive power controlled by the proposed SM-H∞ controller, while a sluggish response time and a high reactive power peak was observed following the change of the active power value (at 1.5 s and 3 s) of the other two controllers (conventional SM and SM fuzzy logic).

As a results, the proposed SM-H∞ controller illustrated an excellent performances compared with the other two controllers even in the presence of DFIG rotor parameter variations. In addition, stability, robustness, and a perfect decoupling between the $d-q$ control axes was ensured through maintaining of such control. Moreover, chattering phenomena was largely reduced when the proposed SM-H∞ controller used.

5 Conclusion

In this study, a robust Sliding Mode H∞ controller was developed to control the generated active and reactive power from the DFIG based on variable speed Wind Energy Conversion System (WECS). The proposed controller leads to improve the control performances of the control algorithm that are based on sliding mode techniques by reducing chattering phenomena under variable wind speed produced by the attractive control part and may lead to instability.

The H∞ control method was used to define the attractive control part of the Sliding Mode control algorithm.

The proposed control scheme was compared with the conventional Sliding Mode as well as the Sliding Mode fuzzy logic controllers. The obtain results illustrated the effectiveness of the proposed SM-H∞ controller even in the presence of time varying reference trajectory, speed changing, and DFIG parameter variations. In addition, chattering phenomena was largely reduced and response time was improved using the proposed SM-H∞ controller. Moreover, stability, robustness, and high decoupling between the control axes was ensured. Finally, the proposed control scheme suggested a good solution to improve the Sliding Mode control algorithm performances applied for power generation systems, which helps to ensure high quality of generated power.

References

[1] Chen, J., Chen, J., Gong, C. "New Overall Power Control Strategy for Variable-Speed Fixed-Pitch Wind Turbines Within the Whole Wind Velocity Range", IEEE Transactions on Industrial Electronics, 60(7), pp. 2652–2660, 2013. https://doi.org/10.1109/TIE.2012.2196901

[2] Li, H., Chen, Z. "Overview of different wind generator systems and their comparisons", IET Renewable Power Generation, 2(2), pp. 123–138, 2008. https://doi.org/10.1049/iet-rpg:20070044

[3] Liserre, M., Cardenas, R., Molinas, M., Rodriguez, J. "Overview of Multi-MW Wind Turbines and Wind Parks", IEEE Transactions on Industrial Electronics, 58(4), pp. 1081–1095, 2011. https://doi.org/10.1109/TIE.2010.2103910

[4] Pati, S., Samantray, S. "Decoupled control of active and reactive power in a DFIG based wind energy conversion system with conventional P-I controllers", In: 2014 International Conference on Circuits Power and Computing Technologies [ICCPCT-2014], Nagercoil, India, 2014, pp. 898–903. https://doi.org/10.1109/ICCPCT.2014.7054793

[5] Saidur, R., Mekhilef, S., Ali, M. B., Safari, A., Mohammed, H. A. "Applications of variable speed drive (VSD) in electrical motors energy savings", Renewable and Sustainable Energy Reviews, 16(1), pp. 543–550, 2012. https://doi.org/10.1016/j.rser.2011.08.020

[6] Mensou, S., Essadki, A., Minka, I., Nasser, T., Idrissi, B. B. "Backstepping Controller for a Variable Wind Speed Energy Conversion System Based on a DFIG", International Journal of Electrical and Computer Engineering, 12(9), pp. 598–604, 2018. https://doi.org/10.5281/zenodo.1474543

[7] Narasipuram, R. P. "Modelling and simulation of automatic controlled solar input single switch high step-up DC-DC converter with less duty ratio", International Journal of Industrial Electronics and Drives, 3(4), pp. 210–218, 2017. https://doi.org/10.1504/IJIED.2017.087611

[8] Loucif, M., Boumediene, A., Mechernene, A. "Nonlinear Sliding Mode Power Control of DFIG under Wind Speed Variation and Grid Connexion", Electrotehnică, Electronică, Automatică (EEA), 63(3), pp. 23–32, 2015. [online] Available at: http://www.eea-journal.ro/ro/d/5/p/EEA63_3_3 [Accessed: 14 January 2019]

[9] Pinto, V. P., Campos, J. C. T., Dos Reis, L. L. N., Jacobina, C. B., Rocha, N. "Robustness and Performance Analysis for the Linear Quadratic Gaussian/Loop Transfer Recovery with Integral Action Controller Applied to Doubly Fed Induction Generators in Wind Energy Conversion Systems", Electric Power Components and Systems, 40(2), pp. 131–146, 2011. https://doi.org/10.1080/15325008.2011.629331

[10] Elmansouri, A., El mhamdi, J., Boualouch, A. "Wind energy conversion system using DFIG controlled by back-stepping and RST controller", In: 2016 International Conference on Electrical and Information Technologies (ICEIT), Tangiers, Morocco, 2016, pp. 312–318. https://doi.org/10.1109/EITech.2016.7519612

[11] Belounis, O., Labar, H. "Fuzzy Sliding Mode Controller of DFIG for Wind Energy Conversion", International Journal of Intelligent Engineering and Systems, 10(2), pp. 163–172, 2017. https://doi.org/10.22266/ijies2017.0430.18

[12] Bourouina, A., Chaker, A., Boudjema, Z., Djahbar, A. "Comparative study between PI, RST and sliding mode controllers of a DFIG supplied by an AC-AC converter for wind energy conversion system", Journal of Electronic and Computer Engineering, 8(2), pp. 7–14, 2015. [online] Available at: http://cjece.ubm.ro/vol/8-2015/n2/1509.07-8202.pdf [Accessed: 10 March 2019]

[13] Ardjoun, S. A. E. M., Abid, M. "Fuzzy sliding mode control applied to a doubly fed induction generator for wind turbines", Turkish Journal of Electrical Engineering & Computer Sciences, 23(6), pp. 1673–1686, 2015. https://doi.org/10.3906/elk-1404-64

[14] Boulâam, K., Boukhelifa, A. "Fuzzy sliding mode control of DFIG power for a wind conversion system", In: 2014 16th International Power Electronics and Motion Control Conference and Exposition, Antalya, Turkey, 2014, pp. 353–358. https://doi.org/10.1109/EPEPEMC.2014.6980518

[15] Patnaik, R. K., Dash, P. K., Mahapatra, K. "Adaptive terminal sliding mode power control of DFIG based wind energy conversion system for stability enhancement", International Transactions on Electrical Energy Systems, 26(4), pp. 750–782, 2016. https://doi.org/10.1002/etep.2105

[16] Castillo, O., Melin, P. "Intelligent Systems with Interval Type-2 Fuzzy Logic", International Journal of Innovative Computing, Information and Control, 4(4), pp. 771–783, 2008.

[17] Narasipuram, R. P., Somu, C., Yadlapalli, R. T., Simhadri, L. S. "Efficiency analysis of maximum power point tracking techniques for photovoltaic systems under variable conditions", International Journal of Innovative Computing and Applications, 9(4), pp. 230–240, 2018. https://doi.org/10.1504/IJICA.2018.095812

[18] Melin, P., Castillo, O. "Intelligent control of complex electrochemical systems with a neuro-fuzzy-genetic approach", IEEE Transactions on Industrial Electronics, 48(5), pp. 951–955, 2001. https://doi.org/10.1109/41.954559

[19] Kairous, D., Wamkeue, R. "DFIG-based fuzzy sliding-mode control of WECS with a flywheel energy storage", Electric Power Systems Research, 93, pp. 16–23, 2012. https://doi.org/10.1016/j.epsr.2012.07.002

[20] Saihi, L., Ferroudji, F., Berbaoui, B., Bakou, Y., Koussa, K., Meguellati, F., Roumani, K. "Hybrid control based on sliding mode fuzzy of DFIG power associated WECS", AIP Conference Proceedings, 2123(1), article ID: 030015, 2019. https://doi.org/10.1063/1.5117046

[21] Khoete, S., Manabe, Y., Kurimoto, M., Funabashi, T., Kato, T. "Robust H-infinity Control for DFIG to Enhance Transient Stability during Grid Faults", In: The World Congress on Engineering and Computer Science, vol. 2, San Francisco, USA, 2016, pp. 725–730. [online] Available at: http://www.iaeng.org/publication/WCECS2016/WCECS2016_pp725-730.pdf [Accessed: 26 March 2019]

[22] Wang, Y., Wu, Q., Gong, W., Gryning, M. P. S. "H∞ Robust Current Control for DFIG-Based Wind Turbine Subject to Grid Voltage Distortions", IEEE Transactions on Sustainable Energy, 8(2), pp. 816–825, 2017. https://doi.org/10.1109/TSTE.2016.2621418

[23] Kahla, S., Sedraoui, M., Soufi, Y., Bechouat, M. "Improved Sliding Mode Controller for Maximum Power Point Tracking of WECS", Electrotechnică, Electronică, Automatică (EEA), 66(1), pp. 29–35, 2018. [online] Available at: http://www.eea-journal.ro/ro/d/5/p/EEA66_1_4 [Accessed: 18 February 2019]

[24] Liu, Y., Wang, Z., Xiong, L., Wang, J., Jiang, X., Bai, G., Li, R., Liu, S. "DFIG wind turbine sliding mode control with exponential reaching law under variable wind speed", International Journal of Electrical Power and Energy Systems, 96, pp. 253–260, 2018. https://doi.org/10.1016/j.ijepes.2017.10.018

[25] Fihakhir, A. M., Bouhamida, M. "Nonlinear Control of a Doubly Fed Induction Generator Driven Wind Turbine", Electrotechnică, Electronică, Automatică (EEA), 64(2), pp. 23–30, 2016. [online] Available at: http://www.eea-journal.ro/ro/d/5/p/EEA64_2_4 [Accessed: 20 February 2019]

[26] Chayaopas, N., Assawinchaichote, W. "H∞ Fuzzy Integral Power Control for DFIG Wind Energy System", International Journal of Electrical and Computer Engineering, 11(5), pp. 547–553, 2017. https://doi.org/10.5281/zenodo.1130547

[27] Hamane, B., Benghanemm, M., Bouzid, A. M., Belabbes, A., Bouhamida, M., Draou, A. "Control for Variable Speed Wind Turbine Driving a Doubly Fed Induction Generator using Fuzzy-PI Control", Energy Procedia, 18, pp. 476–485, 2012. https://doi.org/10.1016/j.egypro.2012.05.059

[28] Gadouche, Z., Belfedal, C., Allaoui, T., Belabbas, B. "Speed-Sensorless DFIG Wind Turbine for Power Optimization Using Fuzzy Sliding Mode Observer", International Journal of Renewable Energy Research, 7(2), pp. 613–621, 2017. [online] Available at: https://mail.ijrer.org/ijrer/index.php/ijrer/article/view/5507 [Accessed: 28 January 2019]

[29] Zribi, M., Alrifai, M., Rayan, M. "Sliding Mode Control of a Variable-Speed Wind Energy Conversion System Using a Squirrel Cage Induction Generator", Energies, 10(5), article ID: 604, 2017. https://doi.org/10.3390/en10050604

[30] Vaish, A., Rastogi, D., Kumar, T. K. S. "GA optimized design of stator voltage oriented integral sliding mode control for DFIG based wind energy conversion system", In: 2017 2nd IEEE International Conference on Recent Trends in Electronics, Information & Communication Technology (RTEICT), Bangalore, India, 2017, pp. 904–909. https://doi.org/10.1109/RTEICT.2017.8256729

[31] Adjoudj, M., Abid, M., Aissaoui, A., Ramdani, Y., Bounoua, H. "Sliding Mode Control of a Doubly Fed Induction Generator for Wind Turbines", Revue Roumaine des Sciences Techniques Série Électrotechnique et Énergétique, 56(1), pp. 15–24, 2011. [online] Available at: http://revue.elth.pub.ro/upload/752384MADJOUDJ.pdf [Accessed: 16 March 2019]

[32] Yang, B., Zhang, X., Yu, T., Shu, H., Fang, Z. "Grouped grey wolf optimizer for maximum power point tracking of doubly-fed induction generator based wind turbine", Energy Conversion and Management, 133, pp. 427–443, 2017. https://doi.org/10.1016/j.enconman.2016.10.062

[33] Abdelmalek, S., Belmili, H., Barazane, L., Abdelkader, L. "A New Robust H∞ Control Power", In: International Conference on Control, Engineering & Information Technology (CEIT'14), Sousse, Tunisia, 2014, pp. 123–128. [online] Available at: http://ipco-co.com/PET_Journal/Papers%20CEIT’14/067.pdf [Accessed: 22 April 2019]

[34] Gahinet, P., Apkarian, P. "Structured H∞ Synthesis in MATLAB", IFAC Proceedings Volumes, 44(1), pp. 1435–1440, 2011. https://doi.org/10.3182/20110828-6-IT-1002.00708

[35] Khedri, J. "Monovariable H_∞ Robust Controller for a Permanent Magnet Synchronous Machine (PMSM)", International Journal of Engineering and Technology (IJET), 7(2), pp. 553–561, 2015. [online] Available at: https://pdfs.semanticscholar.org/4539/550fd9b93dfb5aa04dd8b9add46d3397889a.pdf [Accessed: 13 April 2019]

[36] Ozana, S., Pies, M. "Application of H-infinity Robust Controller on PAC", IFAC Proceedings Volumes, 43(24), pp. 126–131, 2010. https://doi.org/10.3182/20101006-2-PL-4019.00025

[37] Belfedal, C., Gherbi, S., Sedraoui, M., Moreau, S., Champenois, G., Allaoui, T., Denaï, M. A. "Robust control of doubly fed induction generator for stand-alone applications", Electric Power Systems Research, 80(2), pp. 230–239, 2010. https://doi.org/10.1016/j.epsr.2009.09.002

[38] Howlader, A. M., Urasaki, N., Yona, A., Senjyu, T., Saber, Y. A. "Design and Implement a Digital H∞ Robust Controller for a MW-Class PMSG-Based Grid-Interactive Wind Energy Conversion System", Energies, 6(4), pp. 2084–2109, 2013. https://doi.org/10.3390/en6042084

[39] Pintea, A., Christov, N., Borne, P., Popescu, D. "H∞ controller design for variable speed wind turbines", In: 18th International Conference on Control Systems and Computer Science, Bucharest, Romania, 2011, paper ID: hal-00719473. [online] Available at: https://hal.archives-ouvertes.fr/hal-00719473 [Accessed: 21 January 2019]